Journal of Rehabilitation in Civil Engineering 11-1 (2023) 21-42

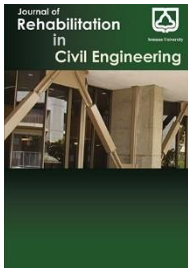

journal homepage: http://civiljournal.semnan.ac.ir/

A Comparative Experimental Study on the Flexural Behavior of Geopolymer Concrete Beams Reinforced with FRP Bars

Sanaz Moazzenchi[1*], Asghar Vatani Oskouei[2]

1. Ph.D. candidate, Department of Structural Engineering, Shahid Rajaee Teacher Training University, Lavizan, PO Box 16785-136, Tehran, Iran.
2. Associate Professor, Department of Structural Engineering, Shahid Rajaee Teacher Training University, Lavizan, PO Box 16785-136, Tehran, Iran.

*Corresponding author: s.moazzenchi@sru.ac.ir

ARTICLE INFO

Article history:
Received: 07 November 2021
Revised: 18 February 2022
Accepted: 19 February 2022

Keywords:
Composite;
FRP;
Geopolymer;
Environment;
Ductility.

ABSTRACT

An environmentally friendly building system with suitable properties including durability can be made by using geopolymer concrete and FRP bars. The flexural behavior of geopolymer concrete beams made from Iran mines soil and reinforced with FRP and steel bars was examined in this work. In terms of reinforcement and concrete, the findings of the experimental investigation of geopolymer concrete beams were compared to those of standard cement concrete beams. To accomplish this purpose, a four-point flexural test was performed on 24 specimens of geopolymer and cement concrete beams reinforced with steel, GFRP, and CFRP bars. The initial cracking load, ultimate load, failure modes, number and width of cracks, load-deflection behavior, crack pattern, strain distribution, effective moment of inertia, and ductility were all investigated. The failure modes of tested beams were approximately similar to those predicted by codes, and a comparison of experimental findings with codes predictions reveals that these codes underestimated the beams' flexural strength, but ACI predictions are almost 20% more accurate than CSA ones. Geopolymer beams reinforced with FRP rebars and made with Iran mine soil showed similar results to reinforced cement beams, and the ductility ratio of FRP and steel reinforced geopolymer beams is 5% and 34% greater than that of reinforced OPC concrete, respectively.

How to cite this article:
Moazzenchi, S., Vatani Oskouei, A. (2023). A Comparative Experimental Study on the Flexural Behavior of Geopolymer Concrete Beams Reinforced with FRP Bars. Journal of Rehabilitation in Civil Engineering, 11(1), 21-42. https://doi.org/10.22075/JRCE.2022.25157.1569

1. Introduction

The steel reinforcements in concrete are protected from corrosion by concrete alkalinity properties. As a consequence, structures are resistant to corrosion and are serviceable. The simultaneous presence of moisture, temperature, and chlorides reduces the alkalinity of concrete which, in turn, gives rise to the corrosion of steel reinforcement inside the concrete. This problem commonly happens in marine structures, parking spaces, and bridges often exposed to violent environments. This corrosion, in turn, damages the concrete and reduces its serviceability. Researchers have suggested using FRP (fiber reinforced polymer) bars made of fibers and impressed in a polymeric resin to resolve the corrosion problems of bars [1]. FRP bars are non-corrosive and nonmagnetic. Thus, they can prevent corrosion and electromagnet interference issues. Furthermore, due to having suitable qualities such as high splitting tensile stress, FRP bars are good choices as reinforcement [2]. Given the issues, including serviceability and economic problems related to rehabilitation and maintenance of structures damaged from corrosion of steel bars, as well as the issue of environmental sustainability and using energy sources in cement and steel production, researchers are trying to find suitable solutions for these problems. Among many solutions, using geopolymer concrete instead of cement concrete and using FRP bars instead of steel ones are effective solutions which have grabbed researchers' attention[3]. After decades of research and practical applications, FRP bars were proposed as a suitable replacement for steel bars as they not only can solve the problem of corrosion, but also have other advantages compared with traditional materials, such as high splitting tensile strength, low weight, easy to use, high durability even in harsh environments, and low costs for maintenance[4–6]. Using of FRP rods has increased in the construction industry in recent years [7]. CFRP and GFRP rebars were studied in many research as reinforcement due to their high tensile strength, high erosion resistance, and durability[8–11]. In particular, Glass Fiber Reinforced Polymer (GFRP) bars are more commonly used to be cost-effective and efficient[12–14]. Beams reinforced with GFRP rebars showed lower flexural strength after cracking than steel- reinforced beams due to the low modulus of elasticity of GFRP[15].

Owning to Geopolymer Cement (GPC) considerable potential compared with OPC, this type of binder came to the researcher's attention. Geopolymer mixture has a comparable performance with traditional cement mixture. The advantage, however, is that it reduces greenhouse gases[16]. The composite action between a GFRP bar and geopolymer concrete definitely occurs because of enough friction resistance of sand coated on GFRP bars and aggregates mechanical interlock [17]. Although many studies were done on the two topics of geopolymer concrete and FRP rebars, few studies are available about combining geopolymer concrete reinforced with FRP bars[18]. Maranan studied on the geopolymer concrete reinforced with FRP rebars and concluded that the beams under flexural and shear stress and the axially loaded columns of geopolymer concrete reinforced with FRP rebars have better or similar mechanical properties to traditional members[19–21]. Studies have also shown that pullout strength and adhesion between GFRP and geopolymer is similar to cement concrete [17,22]. Rangan et al. (2006) [23] maintained that the flexural performance of Geopolymer concrete beams with steel reinforcement is better than similar cement concrete beams, and the behavior and strength of geopolymeric beams containing fly ash are similar to Portland cement beams. Some researchers[24–26] reported that owning to better mechanical properties of geopolymer concrete than OPC, SRGC (steel-reinforced geopolymer concrete) has a better loading capacity compared with comparable RC (reinforced concrete). This performance is better because geopolymer mortar has better bonding than cement mortar. It was reported that the characteristics of geopolymer concrete, such as mechanical strength, dimensional stability, acid resistance, fire resistance, and adhesion between reinforcement and aggregate, are better than cement concrete and also the cost of geopolymer concrete materials is 10 to 30% lower than cement concrete [27]. It was reported that even if the strength of concretes is different, the properties of crack patterns, load-deflection, and failure mode of reinforced geopolymer concrete are analogous to those of reinforced cement concrete[25,26]. Furthermore, it was observed that the chemical bonding of GFRP and concrete increases by the increasing compressive strength of concrete [28]. Maranan et al., (2015) [19] expressed that the bond strength of geopolymer concrete reinforced by GFRP is similar to that of geopolymer concrete reinforced by steel. This was the reason that Maranan proposed that GFRP was a good replacement for reinforcements inside geopolymer concrete structures.

Lack of information about these new materials implies that essential design equations are not sufficient for these bars, and further studies need to be conducted to offer a reliable equation [29]. Due to the lack of a specific standard for geopolymer concrete, standards such as ACI 440.1R-15 [1] and CSA S806-12 [30] were used in the studies, and the accuracy of these regulations was checked. Goonewardena et al. (2020) [31] calculated the error of these regulations below 17% and reported that CSA S806-12[30] was more accurate than the ACI 440.1R-15 [1].

An extensive and reliable database of several experimental applications was collected to develop gene expression programming to investigate the flexural behavior of FRP reinforced beams. This model uses six main parameters that mainly control the flexural behavior of beams, including beam width, concrete compressive strength, beam depth, FRP tensile reinforcement area, FRP modulus of elasticity and ultimate tensile strength of FRP. The predictions of the model were compared with the predictions obtained from the ACI-440 and CSA S806-12 guidelines for further validation of the model. The R-squared values of the three models were very high and close to each other and test results[32].

There have been a few studies on the composition of geopolymer concrete and FRP reinforcement, each of which investigated a specific case, but this study tested and compared all types of GFRP, CFRP, and steel rebars, as well as the cement and geopolymer concrete in the beams, all at the same time and under the same conditions.

Moreover, for the first time, Iran mine zeolite soil and slag of industrial waste were used to make this composition of geopolymer concrete and FRP bars in the beams.

The present study summarized the following purposes:

- To evaluate the flexural response of beams reinforced by GFRP, CFRP, and steel bars under bending test.

- To study the impact of the type of geopolymer and cement concrete in flexural test results; comparing the failure mode, crack pattern, strain, and load-deflection curve.

- Comparing the experimental results with those obtained from ACI440.1R.15 and CSA S806-12 and other researchers' results.

- To study the ductility of beams and affecting factors.

Using reinforced geopolymer concrete with GFRP and CFRP rebars, a building system with high durability, suitable stability, and strength can be built [33].

2. Materials and methods

2.1. Materials

2.1.1. Concrete

Mix design procedures and curing to reach the target strength (30 MPa) for the geopolymer and cement concretes were planned. The geopolymer concrete contained coarse and fine aggregates, water, superplasticizer, and geopolymer paste made from aluminosilicate materials and alkaline solution. For aluminosilicate materials, industrial by-products (blast furnace slag from Isfahan, silica fume) and natural soil (zeolite from Damavand mines in Iran) were used. The chemical compositions of zeolite, slag and silica fume are demonstrated in Table 1. Also, for alkaline liquid, the silicate solution (Na_2SiO_3) and NaOH were utilized. Na_2SiO_3 and NaOH were available in gel and flakes forms, respectively. NaOH flakes were dissolved in water to obtain a 10 molar NaOH solution. Besides, OPC concrete mixture was made of coarse and fine aggregates, water, cement, and superplasticizer. Mix design of samples is given in table 2. Diagrams of coarse and fine aggregates granulation are shown in Fig1.

Table 1. chemical compositions of raw materials.

oxide	SiO_2	Al_2O_3	Fe_2O_3	CaO	MgO	TiO_2	P_2O_5	MnO	Na_2O	K_2O	$L.O.I$	SO_3
zeolite	72.98	11.63	1.29	1.53	0.56	0.18	0.05	0.015	1.89	2.68	6.89	0.02
slag	35.7	9.53	1.2	37	9.5	<0.1	<0.1	0.1	0.4	0.3		<0.1
silicafume	88.7	1.2	1.1	0.8	0.9	<0.1	0.1	0.1	0.7	1	5.02	0.2

Table 2. Mix design of samples.

Type of concrete	aluminosilicate materials (zeolite/slag)	alkaline solution/ Total weight	silica fume/ aluminosilicate materials	Water/ aluminosilicate materials	aggregates/ Total	Coarse aggregate/ fine aggregates
Geopolymer	500 (kg/m^3)	20%	10%	25%	about 60%	65/35
OPC	500 (kg/m^3)			45%	about 60%	65/35

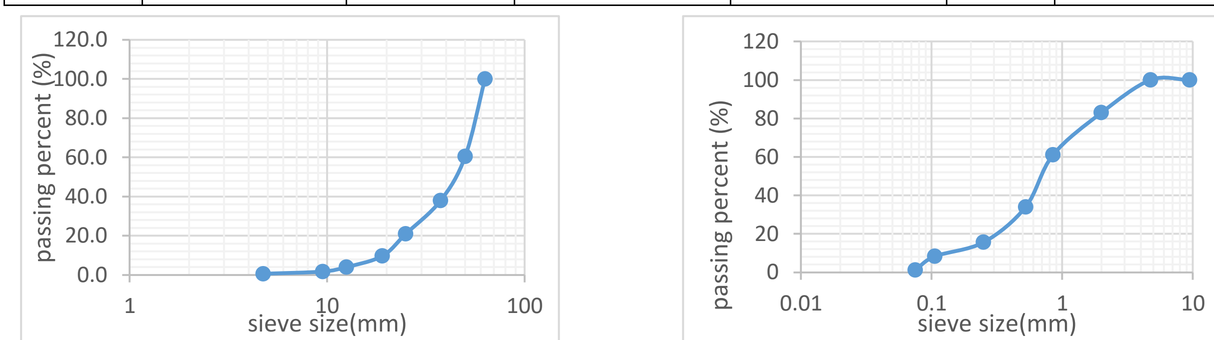

a b

Fig. 1. diagrams of coarse (a) and fine aggregates (b).

2.1.2. Steel and FRP bars

The nominal diameters of used GFRP bars were 10 mm and 12 mm, the diameter of CFRP bars was 6 mm, and the diameters of deformed steel bars used in RC beams were 10 mm and 14 mm. These rods are utilized as tension longitudinal reinforcement. On the other hand, the steel bars with 10 mm and 8 mm diameters were used as compression longitudinal reinforcement and stirrups in all of the tested beams, respectively. Table 3 shows the properties of bars according to manufacturer reports.

Table 3. Specifications of bars.

Reinforcement type	Diameter (mm)	Yield strength (MPa)	Elastic modulus (GPa)	Ultimate strength (MPa)	Elongation rate (%)	Ultimate strain
Steel bar	8	425	205.862	633	28%	0.28
Steel bar	10	417	201.728	601	27%	0.28
Steel bar	14	435	206.149	593	28%	0.28
GFRP bar	10		61	750	1.5%	0.0015
GFRP bar	12		61	1000	2%	0.002
CFRP bar6	6		160	1600	3.5%	0.0035

2.2. Methods

2.2.1. Compressive and tensile strength

The control specimens were tested 28 days after their production, simultaneous with the flexural test day. To be more precise, three cylindrical samples based on ASTMC39 standard [34] were tested for compressive strength, three cylindrical samples based on ASTMC 496 standard [35] were tested for splitting tensile strength, and finally, three ones based on ASTMC 78/C 78M[36] standard were tested for flexural strength.

Furthermore, the elastic modules of GPC were measured by testing three cylindrical samples based on ASTM C469 [35], and its density was calculated via measuring the samples' dimensions and weights. The test results of control samples are given in table 4.

Cylindrical samples were made in the standard size of 150×150×300 mm to measure the samples' splitting tensile strength, compressive strength, and modulus of elasticity. These samples were made from different kinds of concrete i.e., cement concrete and two types of geopolymer concrete with compressive strength of 30 MPa. It was revealed that as compressive strength increases, splitting tensile strength increases as well [37]. This finding is clearly proved in the results of geopolymer concrete shown in Table 4.

Table 4. Results of control samples.

Type of concrete of specimens	Compressive Strength f'_c (Mpa)	Splitting tensile strength f_{ct} (Mpa)	Modulus of Elasticity E_c (Gpa)	Density (kg/m^3)	Strain (mm/mm)
Geopolymer-zeolite	31.6	4.059	21.5	2640	0.0014
Geopolymer-slag	28.1	3.63	23.6	2545	0.0012
OPC	30.5	3.35	31.1	2578	0.001

2.2.2. Flexural test specimens

In this investigation, the flexural test was done for 24 beam specimens by four-point bending test. The samples were designed as simply supported beams with a square cross-section (150mm×150 mm). The total length of the beams was 1200mm. The cover of concrete was 20 mm, and the pure bending length was 350 mm. In all beams, the steel stirrups with a diameter of 8 mm with a center-to-center distance of 70 mm and a 135° hook were used. The arrangement of reinforcements is the same in all beams and is shown in Fig2.

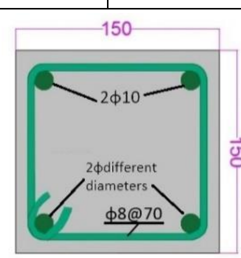

Fig. 2. Arrangement of beams reinforcement.

These specimens were designed as $\rho<\rho_{fb}$ and $\rho>\rho_{fb}$ for comparison. For this purpose, two diameters of rods in types of FRP and steel were chosen. To compare the types of concretes, geopolymer and cement samples were made in each type of reinforcement. This design program is shown in table 5.

Table 6 presents the details of beams and test programs. The geopolymer concrete beams contain zeolite were reinforced with GFRP bars (diameter of 10 mm and 12 mm), steel bars (diameter of 10 mm and 14 mm), and CFRP bars (diameter of 6 mm). To compare the effect of concrete type on flexural strength, two OPC beams reinforced with GFRP12 and steel 14 were produced. Moreover, another type of geopolymer concrete contains slag reinforced with GFRP10 was tested in one of the samples.

Table 5. design program of samples.

ρ (Design)	Reinforcement type	Type of concrete
$\rho < \rho_{fb}$	GFRP10	geopolymer
	CFRP6	geopolymer
	STEEL10	geopolymer
$\rho > \rho_{fb}$	GFRP12	geopolymer
		OPC
$\rho > \rho_{fb}$	STEEL14	geopolymer
		OPC

Table 6. Test program.

group	Beam ID	Concrete type	Compressive Strength- f'_c (Mpa)	*bars*		
				type	D (mm)	ρ (%)
B1	GPC-S10	Geopolymer-zeolite	31.6	STEEL	10	1.39
B2	GPC-S14	Geopolymer-zeolite	31.6	STEEL	14	2.06
B3	GPC-S-G10	Geopolymer-slag	28.1	GFRP	10	1.39
B4	GPC-G10	Geopolymer-zeolite	31.6	GFRP	10	1.39
B5	GPC-G12	Geopolymer-zeolite	31.6	GFRP	12	1.70
B6	GPC-C6	Geopolymer-zeolite	31.6	CFRP	6	0.94
B7	OPC-S14	cement	30.5	STEEL	14	2.06
B8	OPC-G12	cement	30.5	GFRP	12	1.70

2.2.3. Specimen casting and measurement

One day before the production of concrete, the alkaline liquid was prepared. Solid Sodium Hydroxide was first solved in water with the intended concentration (10 molars) to produce it. In fact, 400 grams of this substance dissolving in one liter of water can produce a 10 molar Sodium Hydroxide solution. In the next stage, this solution was mixed with sodium hydroxide solution with the same proportion. This ratio was gained after many trial and error tests to achieve the best result. On casting day, aluminosilicate materials and alkaline liquids were first mixed together so that the geopolymer reactions could occur. Then, aggregates were poured into the mixer. Half of the amount of water was added, and the materials were mixed for five minutes.

Then, the combination of aluminosilicate materials, and the alkaline liquid was added and the mixing process was done for a further five-minute time period. At the end of mixing, the superplasticizer with a weight percentage of 1% and remaining water were added. The newly produced concrete has a shining and dark appearance, as shown in Figure 3.

The four-point static bending test was used to investigate the flexural performance of cement, and geopolymer concretes reinforced with CFRP, GFRP, and steel bars. The load was gradually imposed on the beam with simple support through an I-shaped loaddistributing beam using a hydraulic jack of 1000 kN at a rate of approximately 1 mm/min. To record the length strain of the rebars during the loading process, electrical-resistance strain gauges were installed on the bottom rebars in the midspans of beams. Clear span and shear span of the beams were 350 mm and 350 mm, respectively. A data-logger unit was used to record strain data by connecting it to strain gauges and sensors. Dimensional specifications and test settings of the beams are shown in Figure 4. Moreover, some of the produced beams are shown in Figure 5. Finally, Figure 6 shows one of the beams under the four-point flexural test.

Fig. 3. Appearance of fresh concrete.

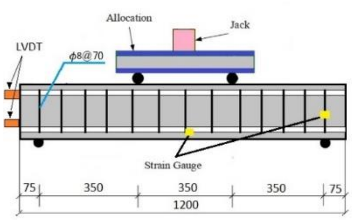

Fig. 4. Test setup.

Fig. 5. A number of beam specimens.

Fig. 6. Four-point bending test.

3. Experimental results and discussion

3.1. Summary of flexure test results

The bending test was performed on the samples, and the results were recorded. The beams' behavior under the loading process, the occurrence of cracks, and the types of beams failure were studied. The first crack in the beams appeared in the constant moment region named 1. After it, new cracks were formed, and as more load was imposed, they started to become wider. All cracks which formed in the beams are shown in figure 7 in order of occurrence time.

Ratios and types of reinforcement and types of concrete substantially affected the load of the first crack and ultimate load of every beam.

These differences also caused changes in the failure mode and cracking pattern. Table 7 presents flexural test results, including first cracking load, ultimate load, failure modes, deflection under ultimate load, and the number and width of cracking. Figure 8 shows the failure moment of the samples in different modes.

When the bending moment exceeded the cracking moment, the first vertical cracks were created and developed within the pure bending-moment zone. As the imposed load increased, the cracks became wider and extended toward the upper part of beam. But shear cracks were also formed along the shear span. Other researchers have similarly stated that the occurred flexural cracks in the mid-span of specimens are formed before the shear cracks [38]. As loading increased, the widths of the vertical cracks in the pure flexural zone increased, then inclined cracks were formed due to shear stress and moved towards the load application points upwards of the sample.

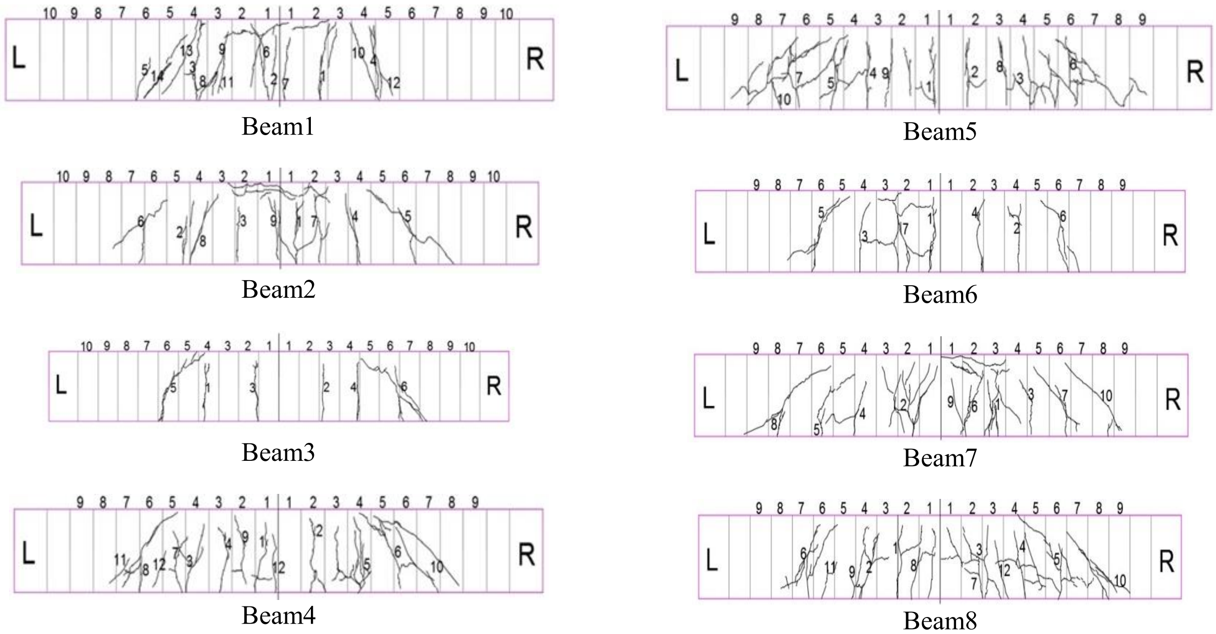

Fig. 7. Crack patterns of beams.

Development of shear inclined cracks moved slowly toward the crushing of concrete in the compression zone, which caused the redistribution of stress in these zones. In the ultimate distribution stage, some inclined cracks had reached the concrete compressive zone. Figure 7 shows the cracking pattern in the tested specimens.

In all beams, cracks were concentrated in the mid-span of beams. The number of cracks was different in the specimens.

Table 7. Results of flexure test.

group	Beam ID	First crack load Pcr (kN)	Ultimate Load Pu (kN)	Deflection (mm)	Failure Mode	Number of cracks	Maximum of crack width (cm)
B1	GPC-S10	20	49.2	63.1	Balance: Bending failure+ Compression failure	13	0.9
B2	GPC-S14	30	92.1	54.5	Compression failure	9	1.2
B3	GPC- S-G10	17	71	40	FRP rupture in shear zone	6	2.2
B4	GPC -G10	12	52.3	24.3	FRP rupture in shear zone	12	1.5
B5	GPC-G12	15	83.9	45.7	Compression failure	10	3.2
B6	GPC-C6	7/5	42.3	20.9	Bending failure	7	2.3
B7	OPC-S14	17	90.2	38	Compression failure	10	3.5
B8	OPC-G12	10	70.4	38	Compression failure	12	3.6

a. Failure mode of beam1

b. Failure mode of beam2

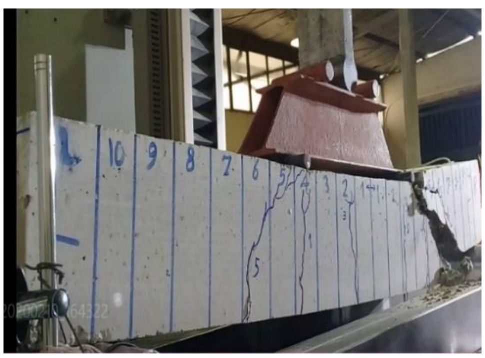

c. Failure mode of beam3

d. Failure mode of beam4

e. Failure mode of beam5

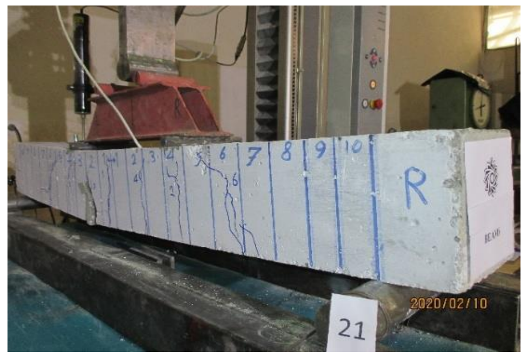

f. Failure mode of beam6

g. Failure mode of beam7

h. Failure mode of beam8

Fig. 8 (a,b,c,d,e,f.g.h). Failure modes of specimens.

3.1.1. First cracking load

When the tensile stress applied to the concrete goes beyond its tensile strength, the concrete begins to crack. Before the cracks occurred, the applied force was tolerated with bars and concrete [39].

According to table 7, the first cracking loads were different in the same concrete types with different reinforcement ratios and types. It shows that the type and amount of reinforcement has an important effect on the first cracking load of beams, same as reported by Qader et al., (2020) [40].

In steel reinforced beams, this factor was higher than that in FRP reinforced beams because of the difference in modulus of elasticity of rods (comparison of beam 1 and beam 4). Also, GPC concrete beams cracked first in higher load than OPC concrete beams (comparison of beam 5 and beam 8, beam 2 and beam7). Hence, it is concluded that the type of concrete also has an important effect on the first cracking load.

3.1.2. Failure Mode and Crack Pattern

The development of cracks in beams occurred in three stages. Step 1: The first crack appeared in the bending area, and gradually the number of cracks and their depth increased. Step 2: The number and depth of cracks more increased, and shear cracks began to form. Step 3: While the number of cracks remained fixed, they slowly started to develop toward the compression zone until the sample failed. Figure 7 shows the pattern of cracking in beams. The patterns of cracks and failure modes are different owning to factors, such as reinforcement percentage, reinforcement type, and concrete type. All tested beams were uncracked before loading. First cracks occurred at the constant moment region.

Beam3(GPC-G10) and beam4(GPC-S-G10) failed because of the rupture of FRP bars under the load in the shape of shear failure. It happened because the stirrups deformed under shear forces, and they forced tension FRP bars, FRP bars were not ductile, so they faced to rupture, while it was designed to FRP rupture in tension. This failure is shown in figure9. Rashid et al. (2020)[41] investigated when FRP rebars are used instead of steel in concrete beams, the beam failure mode changes from flexural to flexural-shear. Failure modes in beams 2(GPC-S14), 5(GPC-G12), 7(OPC-S14), and 8(OPC-G12) were compression failures. This kind of failure was the crushing of concrete in the compression area between two applied loads to the beam. It happened after the tensile bars yielded. Failure mode in beam 1(GPC-S10) happened in balance form, that is, both compression and tension failure happened at one moment. This type of failure is different from the predicting regulations for beam 1 that were designed as $\rho_f < \rho_{fb}$, due according to ACI 318[42] when $\rho_f < \rho_{fb}$, the controlling limit state was the rupture of bars in the tension zone. This proved that the bending rules for geopolymer concrete were slightly different from those for cement concrete and that the provisions of ACI 318 were not entirely accurate. The failure mode for beam 6(G-CFRP6) was because of the rupture of FRP bars in the tension zone. It happened when the reinforcement ratio of beams was in this condition: $\rho_f < \rho_{fb}$.

Fig. 9. Rupture of FRP because of stirrups deforming.

The failure modes of beams 3(GPC-S-G10) and 4(GPC-G10) were the ruptures of FRP bars. It seemed that these specimens failed because of shear failure, but it happened due to the low ductility of FRP bars. After beams deformed, stirrups also deformed and caused damage to FRP bars. Stirrups type and arrangement in all the specimens were the same, but just in the beams with GFRP10 reinforcement, shear failure happened. This result indicates that more stirrups with less distances are required with this type and size of reinforcement.

3.1.3. Number and width of cracks

When the first crack happened in the concrete, the number of cracks increased as the applied load increased. In the next step, increasing the load did not change the number of cracks but increased their width. By less reinforcement ratio, more cracks formed in all types of concrete and bars due to good adhesion to concrete. The number of cracks is given in table 7 and shown in fig 7. The number of cracks in beams 6 (GPC-C6) and 3(GPC-S-G10) was less than other beams due to the high Modulus of Elasticity of CFRP beside the small diameter of this reinforcement and type of geopolymer-slag concrete for proper adhesion between this type of concrete and FRP reinforcement respectively.

The investigation of crack mechanisms in studies showed that there was a close relationship between crack spacing and bonding between concrete and reinforcement [43–48]. Widths of main cracks increased as load increased. The results of crack widths in tested beams are shown in table 7. After tensile bars yielding, the rate of increasing crack width became faster. The formed cracks began to branch and merged with adjacent cracks. At last, horizontal cracks were formed on the concrete.

Crack width values in cement concrete beams were higher than those in geopolymer concrete beams, same as other studies [49]. Increasing the compression strength of the concrete also increased the bonding strength[50]. Results of cracks widths and the number of cracks in beams indicated that the formation of more cracks leads to less crack width and vice versa that table 7 confirms this result.

3.1.4. Load-Deflection relationship

Figure 10 shows the load-deflection curves of tested beams. As the graphs show, all the beams reinforced with FRP bars have two main points. These points are the cracking point and the yield point which was equal to the failure point. After the occurrence of the first crack, the slope of the curves, which is, in fact, its stiffness, reduced. This reduction is more in steel beams and less in FRP ones.

However, samples reinforced with steel bars have a third point called the failure point. In the graphs related to the steel-reinforced beams, three parts can be seen. The first part of the curve is related to the stiffness of non-cracked concrete which is completely linear. The second part pertains to the area after concrete cracking, which is nonlinear. When the first crack happened, the beam stiffness decreased; and as the load increased, the stress of steel bars increased as well until the bars reached the yield resistance. After yielding of steel bars, their stiffness reduced considerably, and the midspan deflection increased quickly.

However, in the samples reinforced with FRP bars, since there is no specific yield point for this type of bar, the curve still remains linear after the first crack until the crushing moment. This result could be seen in Ou et al. (2004) [51] research too. As Figure 10 also indicates, due to the low elasticity module of FRP bars, the slope of the load-deflection curve for steel-reinforced beams is remarkably larger than that for FRP-reinforced ones. After cracking of the concrete, the stiffness of tested beam samples reduced as the number and width of cracks increased. In general, there are two major stages for FRP beams in these graphs.

First, the linear part of the curves with a steep slope is related to the conditions prior to cracking. In this stage, only the concrete sustained the load. Second, when cracking happened in concrete, a drop occurs in the slope of the graph because of the beams' progressive cracks. The number of cracks can be distinguished from these graphs. This part is almost linear except where the cracks occurred, and a sudden drop is seen in the curves. The results showed that the ultimate load of beams increased as the reinforcement rate increased.

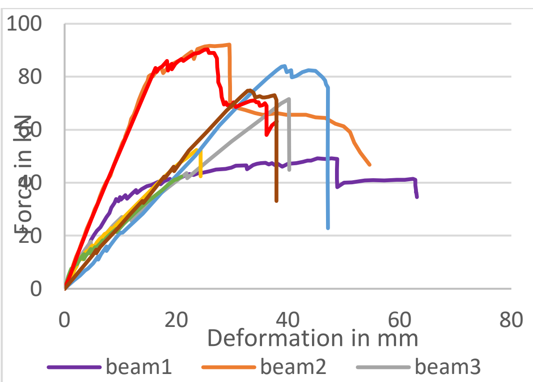

Fig. 10. Load-deflection diagrams.

The mid-span deflection of beam5 (GPC-G12) is 83% less than beam2 (GPC-S14), and the midspan deflections of beam 4(GPC-G10) are 38% less than beam 1 (GPC-S10) in the same load after yield point of steel as shown in table 7. The mid-span deflection of beam 7(OPC-S14) is 69% lower than beam2 (GPC-S14), and the mid-span deflection of beam 8(OPC-G12) is 83% lower than beam5(GPC-G12) in failure load. This characteristic for beam 4(GPC-G10) is also 60% lower than beam3 (GPC-S-G10).

In GPC-GFRP beams, the ultimate loads of beam 4(GPC-G10) are the same as beam 1(GPC-S10). The ultimate load of beam 6(G-CFRP6) is 80% and 85% lower than beams 4(GPC-G10) and 1(GPC-S10), respectively. This slight difference occurs despite the lower reinforcement ratio due to the high tensile strength of CFRP bars. The ultimate load for beam 8(OPC- G10) is 83% lower than beam 5(GPC-G12), and the ultimate loads of beam 2 (GPC-S14) and beam 7 (OPC-S14) are approximately the same in failure. The ultimate loads of the beams for the same type of concrete and reinforcement decreased with an increase in the reinforcement ratio. The ultimate load for beam3(GPC-S-G10) is 35% more than beam 4(GPC-G10) and the same as beam 8(OPC-G10).

As a result, midspan deflection of the steel-reinforced beam is more than FRP reinforced beams after yield point of steel, but the ultimate load of these two types is the same. Furthermore, the midspan deflection of OPC beams is less than GPC ones, but their ultimate load is approximately the same. These results were obtained in other research; Ahmed et al. (2020) [52]stated that the deformation of geopolymer beams reinforced with GFRP is more than cement beams, and the ultimate load of cement concrete is more than geopolymer concrete.

3.1.5. Effect of concrete type

This section studied the effect of the types of concrete (geopolymer concrete with two different materials and cement concrete with equal section and strength given in tables 6 and 7) on the results. The deflection of geopolymer concrete beams was more than the cement concrete beam.

The ultimate load-carrying strength of geopolymer concrete was approximately the same as that of cement concrete. This happened because of the suitable mechanical properties of geopolymer concrete compared with those of cement concrete. Other researchers have similarly reported that the deflection of geopolymer concrete was slightly higher than that of cement concrete and its ultimate load was less than that of cement concrete in equal load conditions[49]. The ultimate deflection and final load of geopolymer concrete made with slag was more than those of geopolymer concrete made with Zeolite soil.

3.1.6. Strain distribution

The strain developments of FRP bars and steel bars in beams are shown in Fig 11. These figures show the strain of bottom longitudinal rods in the middle of the pure bending region. Since the strain gauges in beams 2 and 3 were damaged during the producing process of specimens, the strain results from these beams are not available. Fig 11-a shows the strain-load curves of beams 1 and 7 that are reinforced with steel rods and fig11-b related to beams 4,5,6, and 8 that are reinforced with FRP rods. In fig 11-a the rate of the rapid increase in the pure bending section is related to the steel bar yielding When the load reached the yielding load. The strain of the FRP bars in beams 4,5,6, and 8 remained elastic until they failed and beam 6 failed because of bending failure.

The results also indicate that the strain of FRP reinforcement of beams 5, 6, and 8 reached their ultimate strain, while beam 4 experienced failure before reaching the ultimate strain. This represented the shear failure mode of the concrete beam.

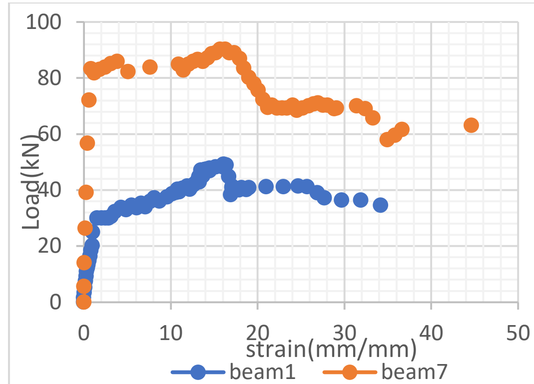

Fig. 11-a. Strain of steel bars in the pure bending moment..

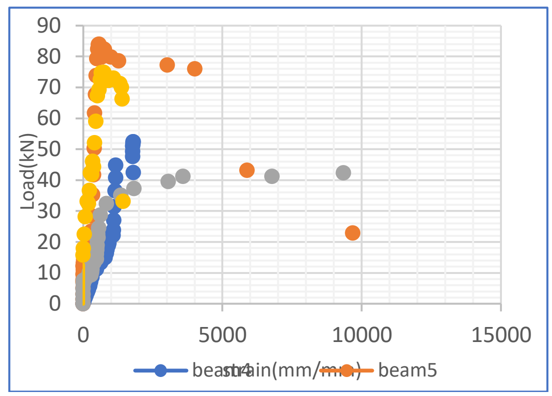

Fig. 11-b. Strain of FRP bars in the pure bending moment.

The failure mode of beam 4(GPC-G10) was the rupture of the FRP bars. As previously explained, it happened due to the low ductility of FRP bars; after beams deformed, stirrups also deformed and caused damage to FRP bars. This can be proved by the strain distribution diagram. It can be seen in this diagram that the GFRP rods did not reach their ultimate strain and failed.

4. Theoretical Prediction

The theoretical flexural capacities (*M*u) of FRP-GPC and FRP-OPC beams were computed according to ACI 440.1R-15[1] and CSA S806-12 [30] equations. These equations can be estimated using as equations in table 8.

Then, these results were compared with the results of experimental flexural capacities (*M*u− exp).

4.1. Experimental results and theoretical predictions comparison

The flexural strength of beams was predicted according to ACI 440.1R-15[1] and CSA S806-12[30]. The results of these predictions are given in table 9. On the other hand, the experimental flexural strength (Mu-Exp) results are shown in this table.

So, in this table, the experimental flexural strength (Mu-Exp) results compare with the prediction of ACI 440.1R-15[1] and CSA S806-12 [30].

Table 8. ACI 440.1R-15 [1] and CSA S806-12 [30] prediction equations.

ACI 440.1R-15		CSA S806-12	
$\rho_{f}=\frac{A_f}{bd}$	(1)	$\rho_{fb}=\alpha_1\beta_1\frac{f_c'}{f_{fu}}\frac{E_f\varepsilon_{cu}}{E_f\varepsilon_{cu}+f_{fu}}$	(8)
$\rho_{fb}=0.85\frac{f'_c}{f_{fu}}\beta_1\frac{E_f\varepsilon_{cu}}{E_f\varepsilon_{cu}+f_{fu}}$	(2)	$\alpha_1=0.85-0.0015f_c'\geq 0.67$	(9)
$f_f=\left[\sqrt{\frac{(E_f\varepsilon_{cu})^2}{4}+\frac{0.85\beta_1 f'_c}{\rho_f}E_f\varepsilon_{cu}}-0.5E_f\varepsilon_{cu}\right]$	(3)	$\beta_1=0.85-0.0025f_c'\geq 0.67$	(10)
$\beta_1=0.85-0.05\frac{f_c'-28}{7}\geq 0.65$	(4)	$M_u=\rho_f f_f bd^2(1-\frac{\rho_f f_f}{2\alpha_1 f_c'}$	(11)
$\rho>\rho_b\rightarrow M_n=\rho_f f_f\left(1-0.59\frac{\rho_f f_f}{f'_c}\right)bd^2$	(5)	$f_f=A_fE_f\frac{\varepsilon_{cu}(d-c)}{c}<f_{fu}$	(12)
$\rho<\rho_b\rightarrow M_n=A_f f_{fu}(d-\frac{B_1c}{2})$	(6)	$\alpha_1\beta_1 f_c'bc-A_fE_f\frac{\varepsilon_{cu}(d-c)}{c}=0$	(13)
$B_1c=\frac{A_f f_f}{0.85bf_c'}$	(7)		

Table 9. Comparison of theoretical prediction based on ACI 440.1R-15[1], CSA S806-12[30] and experimental results.

Group	Beam ID	ρ	ρfb	1.4 ρfb	condition	Mu (kN.m) (exp)	Mu (kN.m) (ACI)	Mu (kN.m) (CSA)	Comparison	
									Mu (ACI) / Mu(exp)	Mu (CSA) / Mu(exp)
B3	GPC-S-G10	0.0083	0.0084	0.0118	ρ ≤ ρfb	18.63	10.655	7.2699	0.57	0.39
B4	GPC-G10	0.0083	0.0084	0.0118	ρ ≤ ρfb	13.72	10.655	7.2699	0.77	0.52
B5	GPC-G12	0.0121	0.0050	0.0070	ρ>1.4 ρfb	22.02	12.063	11.323	0.54	0.51
B6	GPC-C6	0.0029	0.0031	0.0043	ρ < ρfb	11.10	10.691	4.3558	0.96	0.84
B8	OPC-G12	0.0121	0.0084	0.0118	ρ > ρfb	18.48	12.063	11.323	0.65	0.61
average									0.698	0.574

The prediction formulas provided by ACI 440.1R-15[1] and CSA S806-12[30] underestimated the flexural strength of beams compared to the results of experiments. This incompatibility results with ACI 440.1R-15[1] were also obtained in other studies[49,53].

The comparison columns in table 9 show that the averages of results obtained from ACI are more accurate than the CSA.

4.2. Ductility evaluation

4.2.1. Ductility index for RC and FRP beams

For assessing the ductility of steel-reinforced samples, a displacement ductility ratio as an index was offered [53]. As shown in Equation 14, this index is obtained from the ratio of the maximum displacement of midspan to the first yielding deflection of beams. The first yield displacement, Δ_y, corresponds to the tangential intersection of the load-deflection curve continued from the original point and the maximum displacement, Δ_{max} as shown in Figure 12 that this value was obtained from load-deflection diagrams in figure 10. Hence, using the displacement–ductility index can offer a new criterion to predict the behavior of reinforced concrete beams[54].

$$\mu = \frac{\Delta max}{\Delta y} \tag{14}$$

On the other hand, these traditional ductility definitions cannot be directly used for FRP structures. It is, then, necessary to offer a new approach to assess the FRP ductility. Over the past two decades, this effort has been made, which ultimately gave two main approaches to estimate the FRP structures ductility [39]. The present study used the energy-based method, which is stated in the following sections.

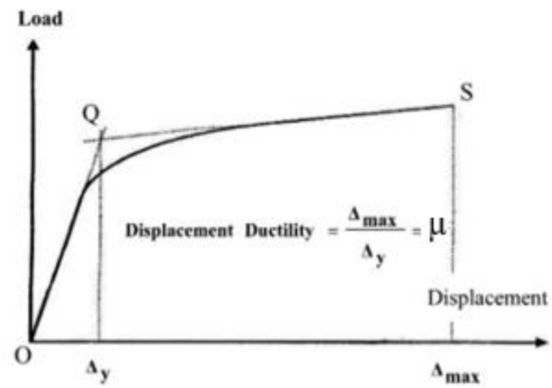

Fig.12. Definition of displacement-ductility ratio of steel reinforced beams[55].

4.2.2. Ductility index by Energy-based approach for FRP beams

In this method, ductility is defined as the capacity of energy absorption. This index is obtained from the ratio of total energy to elastic energy[56]. These components are obtained from the load-deflection curves that are shown in Figure 13. Naaman and Jeong [57] proposed equation 15 to estimate this index.

$$\mu_E = \frac{1}{2}(\frac{E_t}{E_e} + 1) \tag{15}$$

In this equation, E_t is the total energy gained from calculating the underneath surface of the load-deflection curve. E_e is the elastic energy calculated as the area enclosed by the S line. This line is obtained from the failure intersection point, as shown in Figure 13. As the figure clearly reveals, the elastic slope definition depends on choosing points S1, P2, P1, and S2. Although Figure 10 does not clearly show these points, the defined elastic slope equation, S, shown in figure 13, is used to estimate this elastic energy [57].

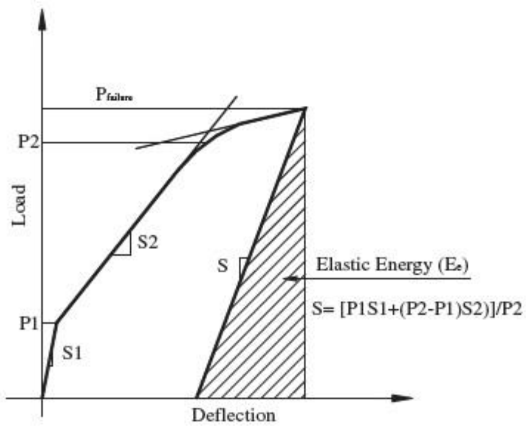

Fig.13. New definition of ductility index of FRP reinforced beams [39].

4.2.3. Discussions of ductility index

As it was explicated in the preceding sections, the ductility index for steel and FRP reinforcements was calculated via two methods whose results are presented in Table 10 and calculated from load-deflections diagrams in figure 10.

Ductility is the ability to absorb energy in materials without losing their loading capacity [39]. Therefore, more energy absorption increases the ductility index [39]. Relevant studies have shown that ductility was different in beams with different FRP reinforcements[58].

According to table 10, the ductility of beams decreases with increasing reinforcement ratios.

This result can be seen in both FRP and steel reinforcement beams. Moreover, the type of concrete has an important effect on ductility; hence, a comparison of B2 and B7, B5 and B8 show that the ductility of geopolymer concrete is more than OPC concrete. Other researchers also reported that increasing the tensile reinforcement ratio results in a lower ductility index. In fact, when the tensile reinforcement ratio in the reinforced concrete beam increases, ductility-deflection index, which represents the samples' ductility, decreases [59]. The results show that the effect of reinforcement type on ductility is more than concrete type.

Table 10. Results of ductility index of beams.

Group	Beam ID	μ-Steel reinforcement	μ_E-FRP reinforcement
B1	GPC-S10	6.8	
B2	GPC-S14	3.4	
B3	GPC- S-G10		2.32
B4	GPC -G10		2.22
B5	GPC-G12		2.1
B6	GPC-C6		3.3
B7	OPC-S14	2.53	
B8	OPC-G12		2

Because the methods of calculating ductility in reinforced beams with steel and FRP rods are different, the results cannot be compared, but some researchers state that the behaviors of FRP reinforced beams are more ductile than the steel- reinforced ones using nonlinear FE analyses[60].

4.3. Effective moment of inertia

When a beam is exposed to load, a bending moment is applied to the beam. Bending stiffness is not constant along the beam, and it varies depending on the applied moment and cracking. If the bending moment is less than the cracking moment, the flexural rigidity of the section remains constant and can be computed using the uncracked inertia, I_g, but if it exceeds the cracking moment, the cracked moment of inertia, I_{cr} is effective in the flexural rigidity calculation [61].

ACI-318-05 [42] expressed the following equation (16) to calculate an effective moment of inertia, I_e for RC beams[62]:

$$I_e = (\frac{M_{cr}}{M_a})^3 I_g + \left[1 - (\frac{M_{cr}}{M_a})^3\right] I_{cr} \leq I_g \quad (16)$$

Where M_a is maximum service moment; M_{cr} is cracking moment; I_g is gross moment of inertia and I_{cr} is cracked moment of inertia.

Due to the lower modulus of elasticity and adhesion stress of FRP than steel bars, ACI 440.1R-06 [63] improved I_e equation for FRP beams by including the reduction coefficient, B_d.

β_d is expressed by:

$$B_d = \frac{1}{5}\left(\frac{p_f}{p_{fb}}\right) < 1 \quad (17)$$

Different studies have provided different relationships for I_e [64–66].

In this study, the effective moment of inertia of the beams according to Equations 16 and 17 are shown in Table 11.

According to the Branson equation, the effective moment of inertia is found at different loading levels between the cracking moment of inertia and the uncracking moment of inertia. In this case, I_e is calculated more than I_{cr}. Results in the table confirm this fact. Results show I_e increases by increasing reinforcement ratio. Hence, I_e in geopolymer concrete is obtained more than that in OPC concrete.

Table 11 Results of effective moment of inertia.

group	I_{cr}(mm^4)	I_e(mm^4)	Type of reinforcement
Beam1	11955522	12285650	Steel10-GPC
Beam2	18945002	18983693	Steel14-GPC
Beam3	4436951	4451234	GFRP10-GPC-slag
Beam4	4436951	4472686	GFRP10-GPC
Beam5	5969295	6000924	GFRP12-GPC
Beam6	4364575	4427172	CFRP6-GPC
Beam7	18945002	18986190	Steel10-GPC
Beam8	5969295	5992320	GFRP10-GPC

5. Conclusion

This research study examined the impact of using different types of concrete (geopolymer and OPC) and reinforcement (steel and FRP bars) on reinforced concrete beams' flexural behavior by using a four-point bending test. The obtained results were then compared with ACI 440.1R-15[1] and CSA S806-12[30] predictions. Based on the experimental and theoretical results, the following findings were obtained:

1. The FRP-reinforced beams were designed in a way that the tension and compression failures happen at reinforcement ratios of $\rho_f < \rho_{fb}$ and $\rho_f > \rho_{fb}$ respectively according to ACI 440.1R-15[1]. Failure modes were almost as predicted.

2. In both steel and FRP reinforced beams, more midspan deformation was recorded with a low reinforcement ratio, and by increasing reinforcement ratio, the more ultimate load was recorded, as expected.
3. The experiments showed that the ultimate loads of OPC and geopolymer beams reinforced with different bars in the same reinforcement ratio were approximately the same. The mid-span deflection of geopolymer concrete beams was about 43% and 20% more than OPC concrete beams in steel and FRP reinforced modes, respectively.
4. The mid-span deflection of GFRP reinforced beams are more than steel-reinforced beams before yielding in the same reinforcement ratio, while the ultimate loads of them were approximately the same.
5. The results of ductility, mid-span deflection, ultimate load, number, and width of crack of geopolymer concrete beam produced with slag were better than geopolymer concrete beam with zeolite due to better adhesion to FRP.
6. In tested beams, low values of crack width were recorded with a large number of cracks. Investigating the number of cracks in beams indicated that the number of cracks in geopolymer concrete samples with slag and also those reinforced with CFRP is less than that in other samples. This can be related to different reasons including the type of slag concrete that has suitable adhesiveness with FRP bars and lower diameter of CFRP bar compared with other bars, and also the high Modulus of elasticity of this bar.
7. Comparing the results of experiments with ACI 440.1R-15[1] and CSA S806-12[30] predictions, it was understood that these codes estimated the flexural strength of reinforced beams differently from those of the experiment results. However, ACI predictions are more acceptable for design the FRP and geopolymer beams, because its predictions are 20% closer to experiment results than CSA ones.

Ductility decreases with increasing reinforcement ratios in both FRP and steel reinforcement beams. Moreover, results showed ductility of geopolymer concrete was more than OPC concrete, the amount of increase in steel reinforced concrete is about 34% and in reinforced concrete with FRP is about 5%.

Conflict of interest

The authors certify that they have NO affiliations with or involvement in any organization or entity with any financial interest.

REFERENCES

[1] ACI Committee 440. ACI440.1R-15 Guide for the Design and Construction of Structural Concrete Reinforced with Firber-Reinforced Polymer (FRP) Bars. vol. 22. 2015.

[2] Thériault M, Benmokrane B. Effects of FRP Reinforcement Ratio and Concrete Strength on Flexural Behavior of Concrete Beams. J Compos Constr 1998;2. https://doi.org/10.1061/(asce)1090-0268(1998)2:1(7).

[3] Maranan GB, Manalo AC, Benmokrane B, Karunasena W, Mendis P. Evaluation of the flexural strength and serviceability of geopolymer concrete beams reinforced with glass-fibre-reinforced polymer (GFRP) bars. Eng Struct 2015;101. https://doi.org/10.1016/j.engstruct.2015.08.003.

[4] Correia JR, Cabral-Fonseca S, Branco FA, Ferreira JG, Eusébio MI, Rodrigues MP. Durability of pultruded glass-fiber-reinforced polyester profiles for structural applications. Mech Compos Mater 2006;42. https://doi.org/10.1007/s11029-006-0042-3.

[5] Bai Y, Post NL, Lesko JJ, Keller T. Experimental investigations on temperature-dependent thermo-physical and mechanical properties of pultruded GFRP composites. Thermochim Acta 2008;469. https://doi.org/10.1016/j.tca.2008.01.002.

[6] Bakis CE, Bank LC, Brown VL, Cosenza E, Davalos JF, Lesko JJ, et al. Fiber-Reinforced Polymer Composites for Construction - State-of-the-Art Review. Perspect. Civ. Eng. Commem. 150th Anniv. Am. Soc. Civ. Eng., 2003. https://doi.org/10.1061/(asce)1090-0268(2002)6:2(73).

[7] Djeddi F, Ghernouti Y, Abdelaziz Y, Alex L. Strengthening in flexure-shear of RC beams with hybrid FRP systems: Experiments and numerical modeling. J Reinf Plast Compos 2016;35. https://doi.org/10.1177/0731684416662532.

[8] Gunasekara C, Law D, Bhuiyan S, Setunge S, Ward L. Chloride induced corrosion in different fly ash based geopolymer concretes. Constr Build Mater 2019;200. https://doi.org/10.1016/j.conbuildmat.2018.12.168.

[9] Al-Majidi MH, Lampropoulos AP, Cundy AB, Tsioulou OT, Alrekabi S. Flexural performance of reinforced concrete beams strengthened with fibre reinforced geopolymer concrete under accelerated corrosion. Structures 2019;19. https://doi.org/10.1016/j.istruc.2019.02.005.

[10] Alzeebaree R, Çevik A, Nematollahi B, Sanjayan J, Mohammedameen A, Gülşan ME. Mechanical properties and durability of unconfined and confined geopolymer concrete with fiber reinforced polymers exposed to sulfuric acid. Constr Build Mater 2019;215:1015–32. https://doi.org/10.1016/j.conbuildmat.2019.04.165.

[11] Goldston MW, Remennikov A, Sheikh MN. Flexural behaviour of GFRP reinforced high strength and ultra high strength concrete beams. Constr Build Mater 2017;131. https://doi.org/10.1016/j.conbuildmat.2016.11.094.

[12] Keller T. Towards Structural Forms for Composite Fibre Materials. Struct Eng Int J Int Assoc Bridg Struct Eng 1999;9. https://doi.org/10.2749/101686699780481673.

[13] Keller T. Recent all-composite and hybrid fibre-reinforced polymer bridges and buildings. Prog Struct Eng Mater 2001;3. https://doi.org/10.1002/pse.66.

[14] Sobrino JA, Pulido MDG, Pulido G. Towards advanced composite material footbridges. Struct Eng Int J Int Assoc Bridg Struct Eng 2002;12. https://doi.org/10.2749/101686602777965568.

[15] Ascione L, Mancusi G, Spadea S. Flexural behaviour of concrete beams reinforced with GFRP bars. Strain 2010;46. https://doi.org/10.1111/j.1475-1305.2009.00662.x.

[16] Duxson P, Fernández-Jiménez A, Provis JL, Lukey GC, Palomo A, Van Deventer JSJ. Geopolymer technology: The current state of the art. J Mater Sci 2007;42. https://doi.org/10.1007/s10853-006-0637-z.

[17] Maranan GB, Manalo AC, Karunasena W, Benmokrane B. Pullout behaviour of GFRP bars with anchor head in geopolymer concrete. Compos Struct 2015;132. https://doi.org/10.1016/j.compstruct.2015.07.021.

[18] Junaid MT, Elbana A, Altoubat S. Flexural response of geopolymer and fiber reinforced geopolymer concrete beams reinforced with GFRP bars and strengthened using CFRP sheets. Structures 2020;24. https://doi.org/10.1016/j.istruc.2020.02.003.

[19] Maranan G, Manalo A, Karunasena K, Benmokrane B. Bond Stress-Slip Behavior: Case of GFRP Bars in Geopolymer Concrete. J Mater Civ Eng 2015;27.

https://doi.org/10.1061/(asce)mt.1943-5533.0001046.

[20] Maranan GB, Manalo AC, Benmokrane B, Karunasena W, Mendis P. Behavior of concentrically loaded geopolymer-concrete circular columns reinforced longitudinally and transversely with GFRP bars. Eng Struct 2016;117. https://doi.org/10.1016/j.engstruct.2016.03.036.

[21] Maranan GB, Manalo AC, Benmokrane B, Karunasena W, Mendis P, Nguyen TQ. Shear behaviour of geopolymer-concrete beams transversely reinforced with continuous rectangular GFRP composite spirals. Compos Struct 2018;187. https://doi.org/10.1016/j.compstruct.2017.12.080.

[22] Tekle BH, Khennane A, Kayali O. Bond behaviour of GFRP reinforcement in alkali activated cement concrete. Constr Build Mater 2017;154. https://doi.org/10.1016/j.conbuildmat.2017.08.029.

[23] Rangan BV, Sumajouw D, Wallah S, Hardjito D. Reinforced low-calcium fly ash-based geopolymer concrete beams and columns. 31st Conf. OUR WORLD Concr. Struct. 16 – 17 August 2006, Singapore Reinf., 2014.

[24] Abraham R, S DR, Abraham V. Strength and Behaviour of Geopolymer Concrete Beams. Int J Innov Res Sci Eng Technol 2013;2.

[25] Dattatreya JK, Rajamane N, Sabitha D, Ambily PS, Nataraja M. Flexural behaviour of reinforced Geopolymer concrete beams. Int J Civ Struct Eng 2011;2:138–59.

[26] Kumaravel S, Thirugnanasambandam S, Jeyasehar CA. Flexural Behavior of Geopolymer Concrete Beams with GGBS. Artic J Struct Eng 2014;VII.

[27] Duxson P, Provis JL, Lukey GC, van Deventer JSJ. The role of inorganic polymer technology in the development of “green concrete.” Cem Concr Res 2007;37. https://doi.org/10.1016/j.cemconres.2007.08.018.

[28] Ashrafi H, Bazli M, Oskouei AV. Enhancement of bond characteristics of ribbed-surface GFRP bars with concrete by using carbon fiber mat anchorage. Constr Build Mater 2017;134:507–19. https://doi.org/10.1016/j.conbuildmat.2016.12.083.

[29] Newman N, Ayoub A, Belarbi A. Development length of straight FRP composite bars embedded in concrete. J Reinf Plast Compos 2010;29. https://doi.org/10.1177/0731684408100262.

[30] CSA. Design and Construction of Building structures with Fibre-Reinforced Polymer. 2017.

[31] Goonewardena J, Ghabraie K, Subhani M. Flexural performance of FRP-reinforced geopolymer concrete beam. J Compos Sci 2020;4. https://doi.org/10.3390/jcs4040187.

[32] Murad Y, Tarawneh A, Arar F, Al-Zu’bi A, Al-Ghwairi A, Al-Jaafreh A, et al. Flexural strength prediction for concrete beams reinforced with FRP bars using gene expression programming. Structures 2021;33. https://doi.org/10.1016/j.istruc.2021.06.045.

[33] Ahmed HQ, Jaf DK, Yaseen SA. Comparison of the Flexural Performance and Behaviour of Fly-Ash-Based Geopolymer Concrete Beams Reinforced with CFRP and GFRP Bars. Adv Mater Sci Eng 2020;2020:1–15. https://doi.org/10.1155/2020/3495276.

[34] ASTM C39/C39M. Standard Test Method for Compressive Strength of Cylindrical Concrete Specimens 1. ASTM Stand B 2003;i.

[35] ASTM C496. Standard Test Method for Splitting Tensile Strength of Cylindrical Concrete Specimens. Man Hydrocarb Anal 6th Ed 2008.

[36] AMERICAN SOCIETY FOR TESTING AND MATERIALS (ASTM). Astm C78. vol. 04.02. 2002.

[37] Mermerdaş K, Manguri S, Nassani DE, Oleiwi SM. Effect of aggregate properties

on the mechanical and absorption characteristics of geopolymer mortar. Eng Sci Technol an Int J 2017;20. https://doi.org/10.1016/j.jestch.2017.11.009.

[38] Oskouei AV, Kivi MP, Araghi H, Bazli M. Experimental study of the punching behavior of GFRP reinforced lightweight concrete footing. Mater Struct Constr 2017;50. https://doi.org/10.1617/s11527-017-1127-2.

[39] Wang H, Belarbi A. Ductility characteristics of fiber-reinforced-concrete beams reinforced with FRP rebars. Constr Build Mater 2011;25:2391–401. https://doi.org/10.1016/j.conbuildmat.2010.11.040.

[40] Ahmed HQ, Jaf DK, Yaseen SA. Flexural strength and failure of geopolymer concrete beams reinforced with carbon fibre-reinforced polymer bars. Constr Build Mater 2020;231. https://doi.org/10.1016/j.conbuildmat.2019.117185.

[41] Rashid K, Li X, Xie Y, Deng J, Zhang F. Cracking behavior of geopolymer concrete beams reinforced with steel and fiber reinforced polymer bars under flexural load. Compos Part B Eng 2020;186. https://doi.org/10.1016/j.compositesb.2020.107777.

[42] ACI Committee 318. ACI 318/318R-05: Building Code Requirements for Structural Concrete and Commentary. Aci 318-05 2005;2003.

[43] Visintin P, Oehlers DJ, Muhamad R, Wu C. Partial-interaction short term serviceability deflection of RC beams. Eng Struct 2013;56. https://doi.org/10.1016/j.engstruct.2013.06.021.

[44] Yankelevsky DZ, Jabareen M, Abutbul AD. One-dimensional analysis of tension stiffening in reinforced concrete with discrete cracks. Eng Struct 2008;30. https://doi.org/10.1016/j.engstruct.2007.03.013.

[45] Visintin P, Oehlers DJ, Wu C, Haskett M. A mechanics solution for hinges in RC beams with multiple cracks. Eng Struct 2012;36. https://doi.org/10.1016/j.engstruct.2011.11.028.

[46] Oehlers DJ, Mohamed Ali MS, Haskett M, Lucas W, Muhamad R, Visintin P. FRP-Reinforced Concrete Beams: Unified Approach Based on IC Theory. J Compos Constr 2011;15. https://doi.org/10.1061/(asce)cc.1943-5614.0000173.

[47] Marti P, Alvarez M, Kaufmann W, Sigrist V. Tension Chord Model for Structural Concrete. Struct Eng Int J Int Assoc Bridg Struct Eng 1998;8. https://doi.org/10.2749/101686698780488875.

[48] Muhamad R, Mohamed Ali MS, Oehlers D, Hamid Sheikh A. Load-slip relationship of tension reinforcement in reinforced concrete members. Eng Struct 2011;33. https://doi.org/10.1016/j.engstruct.2010.12.022.

[49] Khaneghahi MH, Najafabadi EP, Shoaei P, Oskouei AV. Effect of intumescent paint coating on mechanical properties of FRP bars at elevated temperature. Polym Test 2018;71. https://doi.org/10.1016/j.polymertesting.2018.08.020.

[50] Doost Mohamadi A, Vatani Oskouei A, Kheyroddin A. An experimental study on effect of concrete type on bond strength of GFRP bars. J Rehabil Civ Eng 2021;9. https://doi.org/10.22075/JRCE.2020.19922.1392.

[51] Ou J, Wang B, He Z, Zhang X, Qian M. Load-deflection response of concrete beams reinforced with FRP bars. Adv Struct Eng 2004;7. https://doi.org/10.1260/1369433042863242.

[52] Ahmed HQ, Jaf DK, Yaseen SA. Flexural Capacity and Behaviour of Geopolymer Concrete Beams Reinforced with Glass Fibre-Reinforced Polymer Bars. Int J Concr Struct Mater 2020;14. https://doi.org/10.1186/s40069-019-0389-1.

[53] Annamalai S, Thirugnanasambandam S, Muthumani K. Flexural behaviour of geopolymer concrete beams cured under ambient temperature. Asian J Civ Eng 2017;18.

[54] Rakhshanimehr M, Esfahani MR, Kianoush MR, Mohammadzadeh BA, Mousavi SR. Flexural ductility of reinforced concrete beams with lap-spliced bars. Can J Civ Eng 2014;41. https://doi.org/10.1139/cjce-2013-0074.

[55] Azizinamini A, Pavel R, Hatfield E, Ghosh SK. Behavior of lap-spliced reinforcing bars embedded in high-strength concrete. ACI Struct J 1999;96. https://doi.org/10.14359/737.

[56] Yoo DY, Banthia N, Yoon YS. Predicting the flexural behavior of ultra-high-performance fiber-reinforced concrete. Cem Concr Compos 2016;74. https://doi.org/10.1016/j.cemconcomp.2016.09.005.

[57] Taerwe L. Structural ductility of concrete beams prestressed with FRP tendons. Non-Metallic Reinf. Concr. Struct., 2020. https://doi.org/10.1201/9781482271621-56.

[58] Zhu H, Cheng S, Gao D, Neaz SM, Li C. Flexural behavior of partially fiber-reinforced high-strength concrete beams reinforced with FRP bars. Constr Build Mater 2018;161. https://doi.org/10.1016/j.conbuildmat.2017.12.003.

[59] Mohammadhassani M, Suhatril M, Shariati M, Ghanbari F. Ductility and strength assessment of HSC beams with varying of tensile reinforcement ratios. Struct Eng Mech 2013;48. https://doi.org/10.12989/sem.2013.48.6.833.

[60] Shirmardi M, Mohammadizadeh M. Numerical Study on the Flexural Behaviour of Concrete Beams Reinforced by GFRP Bars. J Rehabil Civ Eng 2019;7:88–99.

[61] Nanni A, De Luca A, Zadeh H. Reinforced Concrete with FRP Bars: Mechanics and Design. 2014.

[62] Branson DE, Metz GA. Instantaneous and time-dependent deflections of simple and continuous reinforced concrete beams. 318Reference 1963;9.

[63] ACI 440.1R-06. Guide for the design and construction of concrete reinforced with FRP bars. Am Concr Inst 2006.

[64] Faza S, GangaRao H. Pre- and post-cracking deflection behaviour of concrete beams reiforced with fibre-reinforced plastic rebars. Proc ICUACMBS Can Soc Civ Eng 1992.

[65] Toutanji HA, Saafi M. Flexural behavior of concrete beams reinforced with glass fiber-reinforced polymer (GFRP) bars. ACI Struct J 2000;97. https://doi.org/10.14359/8806.

[66] Rafi MM, Nadjai A. Evaluation of ACI 440 deflection model for fiber-reinforced polymer reinforced concrete beams and suggested modification. ACI Struct J 2009;106. https://doi.org/10.14359/51663177.